Geophysical Journal International

Geophys. J. Int. (2016) **204,** 785–797 doi: 10.1093/gji/ggv485
GJI Geomagnetism, rock magnetism and palaeomagnetism

Geomagnetic palaeosecular variation around 15 ka ago from NW Barents Sea cores (south of Svalbard)

Leonardo Sagnotti,[1] Patrizia Macrì[1] and Renata G. Lucchi[2]

[1] *Istituto Nazionale di Geofisica e Vulcanologia, Roma, Italy. E-mail: leonardo.sagnotti@ingv.it*
[2] *Istituto Nazionale di Oceanografia e di Geofisica Sperimentale, Borgo Grotta Gigante, Sgonico, Trieste, Italy*

Accepted 2015 November 5. Received 2015 November 5; in original form 2015 February 27

SUMMARY

The sedimentary sequence deposited during the deglaciation phase following the last glacial maximum in the Storfjorden trough, on the northwestern Barents Sea south of Svalbard, was sampled with 10 piston and gravity cores during the SVAIS and EGLACOM cruises. Three cores (SV-02, SV-03 and SV-05) collected on the upper continental slope are characterized by a thin (20–40 cm) Holocene interval and a thick (up to 4.5 m in core SV-03) late Pleistocene sequence of finely laminated fine-grained sediments that have been interpreted as plumites deposited during the Melt Water Pulse 1a (MWP-1a). Radiocarbon ages obtained at the top and bottom of this stratigraphic interval revealed that deposition occurred during less than two centuries at around 15 ka ago, with a very high sedimentary rate exceeding 3 cm a^{-1}. We studied the palaeomagnetic and rock magnetic properties of this interval, by taking magnetic measurements at 1 cm spacing on u-channel samples collected from the three cores. The data show that this sequence is characterized by good palaeomagnetic properties and the palaeomagnetic and rock magnetic trends may be correlated at high resolution from core to core. The obtained palaeomagnetic data therefore offer the unique opportunity to investigate in detail the rate of geomagnetic palaeosecular variation (PSV) in the high northern latitudes at a decadal scale. Notwithstanding the palaeomagnetic trends of the three cores may be closely matched, the amplitude of directional PSV and the consequent virtual geomagnetic pole (VGP) scatter (S) is distinctly higher in one core (SV-05) than in the other two cores (SV-02 and SV-03). This might result from a variable proportion of two distinct populations of magnetic minerals in core SV-05, as suggested by the variable tendency to acquire a gyromagnetic remanent magnetization at high fields during the AF demagnetization treatment. For the plumite interval of cores SV-02 and SV-03, where the magnetic mineralogy is uniform and magnetite is the main magnetic carrier, a *S* value of about 9° is obtained. We consider this value as a reliable approximation of palaeomagnetic secular variation at a latitude of 75°N over a time interval spanning a couple of centuries around 15 ka ago.

Key words: Palaeomagnetic secular variation; Rock and mineral magnetism; Arctic region.

INTRODUCTION

The spectrum of Earth's magnetic field variation spans a very broad timescale, ranging from milliseconds to hundreds of million years. Geomagnetic variations with a duration longer than *ca*. 5 a are collectively defined as secular variation (SV; Thompson & Barraclough 1982; Bloxham & Gubbins 1985). The variations developing over time intervals longer than 22 a (i.e. the duration of the periodic turnover of solar magnetic field) are of internal origin and are caused by the flow in the Earth's fluid outer core and from effects of magnetic field diffusion in the core and the mantle (e.g. Bullard 1948; Holme & Olsen 2006).

The reconstruction of the secular variation of the geomagnetic field in the geological past (known as palaeosecular variation—PSV) relies upon palaeomagnetic methods (Creer 1962, 1981). The establishment of master regional PSV curves (Turner & Thompson, 1981, 1982; Hagstrum & Champion 2002; Snowball *et al*. 2007) then allows to use individual PSV curves as an original tool to date both sedimentary (Verosub 1988; Sagnotti *et al*. 2011a,b) and lava (Tanguy *et al*. 1985; Holcomb *et al*. 1986; Speranza *et al*. 2008) sequences of the Holocene and the late Quaternary.

Several studies were carried out on PSV of the geomagnetic field, with the aim to understand its statistical behaviour averaged over various time intervals and to define its geographic variability.

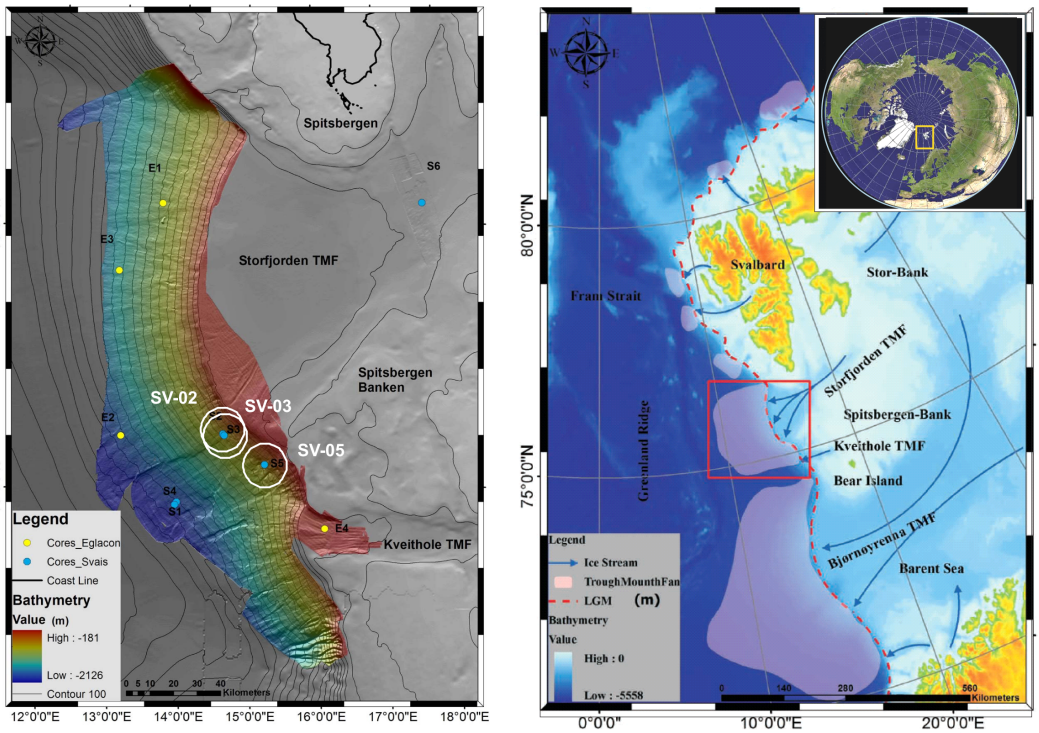

Figure 1. Location map of the study area in the NW Barents Sea, with indication of the SVAIS (S) and EGLACOM (E) cores. The three cores selected for this study (SV-02-SV-03 and SV-05) are marked by white circles. The Storfjorden through was shaped by the action of palaeo-ice streams that flowed periodically through it, originating from the southern Svalbard archipelago and Spitsbergen banken.

In particular, many studies focused on the variation of geomagnetic angular dispersion with latitude (e.g. Creer *et al*. 1959; Cox 1970; Lund 1985; Constable & Parker 1988; McFadden *et al*. 1988; Vandamme 1994; Biggin *et al*. 2008; Deenen *et al*. 2011).

Studies on PSV are based on the assumption that sediments and lavas are faithful recorders of the past geomagnetic field, which is a hypothesis not always verified and verifiable. We here present new palaeomagnetic data from a sequence of interlaminated sediments deposited by subglacial outbursts of turbid meltwaters (plumites) retrieved from three adjacent piston cores from the upper slope of the north-western Barents Sea. These data provide the opportunity to investigate and compare PSV trends recorded in sediments from high northern latitude at an unprecedented resolution. A massive terrigenous input associated to an outstanding meltwater event during the last deglaciation, generated a several meter-thick plumitic interval settled in less than two centuries with an extreme sedimentation rate of 3.4 cm a^{-1} (Lucchi *et al*. 2013).

The Holocene interval of the same sedimentary sequence is characterized by reliable palaeomagnetic properties, with PSV and relative palaeointensity (RPI) curves replicable between distinct cores, that allowed development of a directional and intensity stack for the region (Sagnotti *et al*. 2011b).

In this study, we present the palaeomagnetic data from the plumites interval from three cores (SV-02, SV-03 and SV-05) and discuss their bearing on the accuracy and significance for the establishment of reliable PSV models.

GEOLOGICAL SETTING, DEPOSITIONAL PROCESSES AND CORE STRATIGRAPHY

The sedimentary system of the Storfjorden and Kveithola Trough Mouth Fans (TMFs) on the northwestern Barents Sea south of Svalbard was investigated within the projects SVAIS, NICESTREAMS-Spain and OGS-EGLACOM, the Spanish and OGS (Italy) contributions to IPY Activity N. 367 (NICESTREAMS; Fig. 1).

Trough-mouth fans (TMF) are sedimentary depocentres located at the mouth of cross-shelf glacial troughs on continental shelves (Vorren & Laberg 1997; Taylor *et al*. 2002). They represent sites of significant detrital sediment accumulation during glacial maxima when ice streams reach the outer continental shelf. The onset of the northern hemisphere glaciation and the progressive expansion of the Barents Sea Ice Sheet on the continental shelf have determined rapid accumulation of diamicton from glacially driven debris flows alternated with interglacial glacimarine sedimentation (Laberg & Vorren 1996). According to Rebesco *et al*. (2013), the onset and development of TMFs in the South-western Svalbard margin occurred since 1.3 Ma.

The sedimentary sequence of the piston and gravity cores recovered during the SVAIS and EGLACOM cruises contains the record of last deglaciation including, in some cases, the Last Glacial Maximum (LGM). The Holocene sequence consists of heavily bioturbated and crudely laminated fine-grained sediments (*contourites*) on the middle slope and IRD-rich, bioturbated sediments on the upper slope and outer shelf area, having thickness of 1–2.5 m (middle slope) and 0.4–1.8 m on the upper slope and continental shelf where, however, it contains several hiatuses. The Holocene sequence of the middle slope cores shows reliable palaeomagnetic properties that allowed the reconstruction of the PSV of the geomagnetic field at high-resolution (Sagnotti *et al*. 2011b). The cores collected on the upper slope are constituted by a thick (up to 4.5 m in core SV-03) late Pleistocene sequence of finely laminated fine-grained sediments interbedded with thin sandy layers (*deglaciation* interval in Fig. 2). This stratigraphic interval was related to subglacial meltwater release of detritus with contour currents reworking of the finer fraction (*plumites sensu* Hesse *et al*. 1997; Lucchi *et al*.

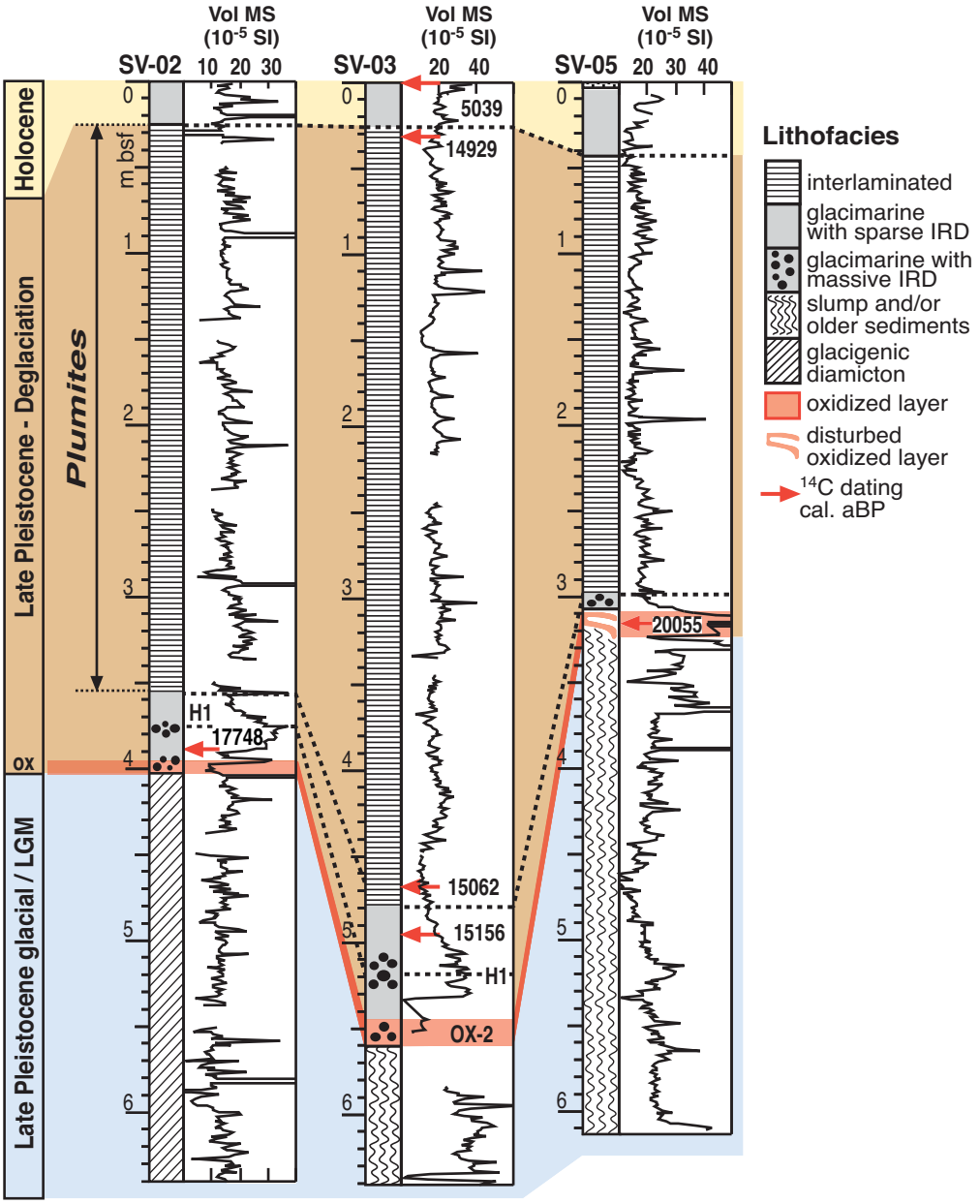

Figure 2. Lithologic logs, AMS 14C calibrated ages and correlation of the EGLACOM and SVAIS cores. The Holocene sequence of the Mid Slope cores provided a high-resolution record of geomagnetic palaeosecular variation (Sagnotti *et al.* 2011b). The present study refers to the SV-02, SV-03 and SV-05 cores of the Upper Slope, which show a thick interval of laminated silty-clays, with a layer of massive fine-grained sediment with sparse IRD (*deglaciation* interval, coloured in brown) which has been deposited in *ca*. two centuries around 15 ka BP, according to the available radiocarbon ages.

2002; Lucchi & Rebesco 2007). Radiocarbon ages obtained at the top and bottom of this facies revealed that the plumites deposited in less than two centuries (Lucchi *et al*. 2013). This interval cannot have been deposited by instantaneous turbidity currents because of the presence of sparse and layered IRD in the finely laminated sediments (see discussion in Lucchi *et al*. 2013). According to the stratigraphic location and radiocarbon ages this exceptionally short living plumite event was indicated to represent the high latitude marine record of Melt Water Pulse 1a (MWP-1a, Lucchi *et al*. 2013). Below this interval, the presence of coarse, massive Ice Rafted Debris (IRD) and an oxidized layer (OX-2) were associated to the initial phase of deglaciation with lift-off of the Ice-sheet and release of fresh, oxygenated water, that was inferred to occur in this area between 20 and 19 cal. ka BP (Lucchi *et al*. 2013).

METHODS

The samples analysed in this study were collected from the undisturbed archive halves of the cores SV-02, SV-03 and SV-05, containing an expanded record of the *deglaciation* interval (Fig. 2). We sub-sampled each core section—about 1 m long—with u-channel plastic holders. On each u-channel, palaeomagnetic and rock magnetic measurements were carried out at 1 cm spacing, with specific instrumentation installed in the magnetically shielded room of the Istituto Nazionale di Geofisica e Vulcanologia palaeomagnetic laboratory. For each u-channel, we first measured the low-field magnetic susceptibility (k) and the natural remanent magnetization (NRM).

The NRM was measured on a small access (45 mm diameter) automated pass-through '2 G Enterprises' DC 755 superconducting

Table 1. Radiocarbon dating.

Sample ID	Lab ref.	Sample type	Description	Process	Raw AMS ^{14}C	Age err.	∂13C	Cal. a BP
SV2-5-39/40	OS-77655	Foraminifera	benthic + planktonic	HY	15050	50	−0.24	17748 ± 139
SV3-1-0/1	OS-77656	Foraminifera	benthic + planktonic	HY	4860	30	−0.07	5039 ± 87
SV3-1-32/33	OS-82683	Mollusc	bivalve	HY	13000	45	1.09	14929 ± 141
SV3-6-21/30	OS-82684	Forams & Ostracods	benthic + plankt. + ostrac.	HY	13200	50	−0.85	15061 ± 146
SV3-6-52/53	OS-77680	Foraminifera	benthic + planktonic	HY	13300	50	−0.4	15156 ± 117
SV5-4-82/83	OS-82689	Foraminifera	Mix plankt. mostly Nps	HY	17350	85	−0.08	20055 ± 166

Note: Nps, Neogloboquadrina pachyderma (s); HY, hydrolysis.

rock magnetometer (SRM) equipped with three orthogonal Superconducting Quantum Interference Devices (SQUID) sensors, while k was measured using a Bartington magnetic susceptibility meter equipped with probe MS2C and mounted in-line with the SRM translating system.

For the NRM measurements, possible spurious effects that may arise from the different shape and widths of the response function curves of the three SQUID pick-up coils (Roberts 2006) were corrected directly by the measuring software, by normalizing the magnetic signal recorded by each pick-up coil by the area under the respective response curve (Weeks *et al*. 1993). This correction compensates for the effects of the negative regions on the edge of the response functions for the transverse axes and for the broader width of the response function along the long axis of the u-channel. In the SRM used for the measurements, the half-width of the SQUID response function is of about 4.1 cm for the transversal components (X and Y) and of about 6.7 cm for the axial component (Z). The computed palaeomagnetic data are therefore free from artefacts that may arise from uncompensated raw magnetic moment data and could result in fictitious inclination shallowing (or steepening) of the palaeomagnetic data (Roberts 2006). In order to avoid edge effects due to the actual width of the SQUID response functions, we disregarded the palaeomagnetic data for <5 cm at both ends of each u-channel and stratigraphic gap.

After measuring the magnetic susceptibility, the NRM was progressively subjected to alternating field (AF) demagnetization in nine steps up to a maximum peak field of 100 mT (steps: 0, 10, 20, 30, 40, 50, 60, 80 and 100 mT), by translating the samples through a set of three orthogonal AF demagnetizing coils in-line with the SRM, with NRM vectors measured after each demagnetization step.

For each u-channel, after the NRM demagnetization cycle, an anhysteretic remanent magnetization (ARM) was imparted applying an axial 0.1 mT bias direct current (DC) field and a simultaneous symmetric AF peak of 100 mT along the SRM translation axis (Z axis in specimen coordinates), while the u-channel was translated through the AF and DC coil system at a constant speed of 10 cm s^{-1}, that is the lowest speed allowed by the measuring software. The adopted procedure equals an AF decay rate of *ca*. 67 μT/half-cycle and results in the highest ARM intensity achievable with the employed instrumental setting and management software (Sagnotti *et al.* 2013).

Since both the NRM and the ARM are almost single component magnetic remanences the median destructive field for each core interval measured was automatically computed from AF demagnetization curves (MDF_{NRM} and MDF_{ARM}, respectively). The MDF is defined as the value of the peak AF necessary to reduce the remanence intensity to half of its initial value and it is a coercivity-dependent magnetic parameter.

Finally, the ΔGRM/ΔNRM ratio provides a quantitative measure of the tendency to acquire a spurious gyromagnetic remanent magnetization (GRM) at high AF steps (Fu *et al*. 2008). ΔGRM represents the difference of the final intensity measured at the last applied AF step and the intensity minimum value (MV) measured during the whole AF treatment; ΔNRM represents the difference of initial intensity value and MV.

Samples for radiocarbon dating were collected at the base and top of the studies interval for chronological constrain. Dating was mostly carried out on a mixture of benthic and planktonic foraminifera, ostracods and on a shell fragment located in the upper part of the interlaminated sequence recovered in core SV-03 (details in Table 1 and in Lucchi *et al*. 2013). Age calibrations were performed using the Calib 6.0 calibration software program (Stuiver & Reimer 1993), applying the marine09 calibration curve (Reimer *et al*. 2009), with an average marine regional reservoir effect $\Delta R = 84 \pm 23$ obtained from the Marine Reservoir Correction Database of the software Calib 6.0 for the northwestern Barents Sea area (data from Mangerud & Gulliksen 1975). The mean values from the calibrated age range of $\pm 1\sigma$ were then normalized to calendar year and will be indicated as cal. a BP (or cal. ka BP).

RESULTS

The analysed cores are characterized by well defined palaeomagnetic properties. The stepwise demagnetization data have been visualized and analysed with the DAIE software (Sagnotti 2013). Each measured interval show an almost single-component NRM: after the removal of a low-coercivity component at 5–10 mT, the palaeomagnetic direction remains remarkably stable up to 50–60 mT, with demagnetization vectors aligned along linear paths towards the origin in orthogonal vector diagrams (Fig. 3). Therefore, a clear and well-defined characteristic remanent magnetization (ChRM) has been isolated for each measurement interval and its direction computed by principal component analysis (Kirschvink 1980) using four consecutive steps at AF peak values between 20 and 50 mT, and the maximum angular deviation (MAD) was computed for each determined ChRM direction.

In the stratigraphic interval of interest (*deglaciation* interval in Fig. 2) the intensity of the NRM shows limited oscillation with values around 0.5–1 × 10^{-2} A m^{-1} in the plumites interval, and a distinct increase up to about 3 × 10^{-2} A m^{-1} in the structureless mud with massive IRD and the underlying OX2 layer. The ARM trend essentially replicates the NRM trend (Fig. 4a). The NRM, ARM and k stratigraphic profiles show common features between the three cores that were used as tie-points to correlate them at high-resolution and to transfer rock magnetic and palaeomagnetic data to a common (SV-03) depth scale (Fig. 5), indicating a substantial reproducibility of data between cores. As stated above, the ChRM directions are mostly very well defined with average MAD values of the order of 2–5° for all the cores (Fig. 4b). The ChRM inclination mostly oscillates in the range 60–70° (Fig. 4b), which is lower than the expected value (about 82°) for a geocentric axial dipole field (GAD) at the high

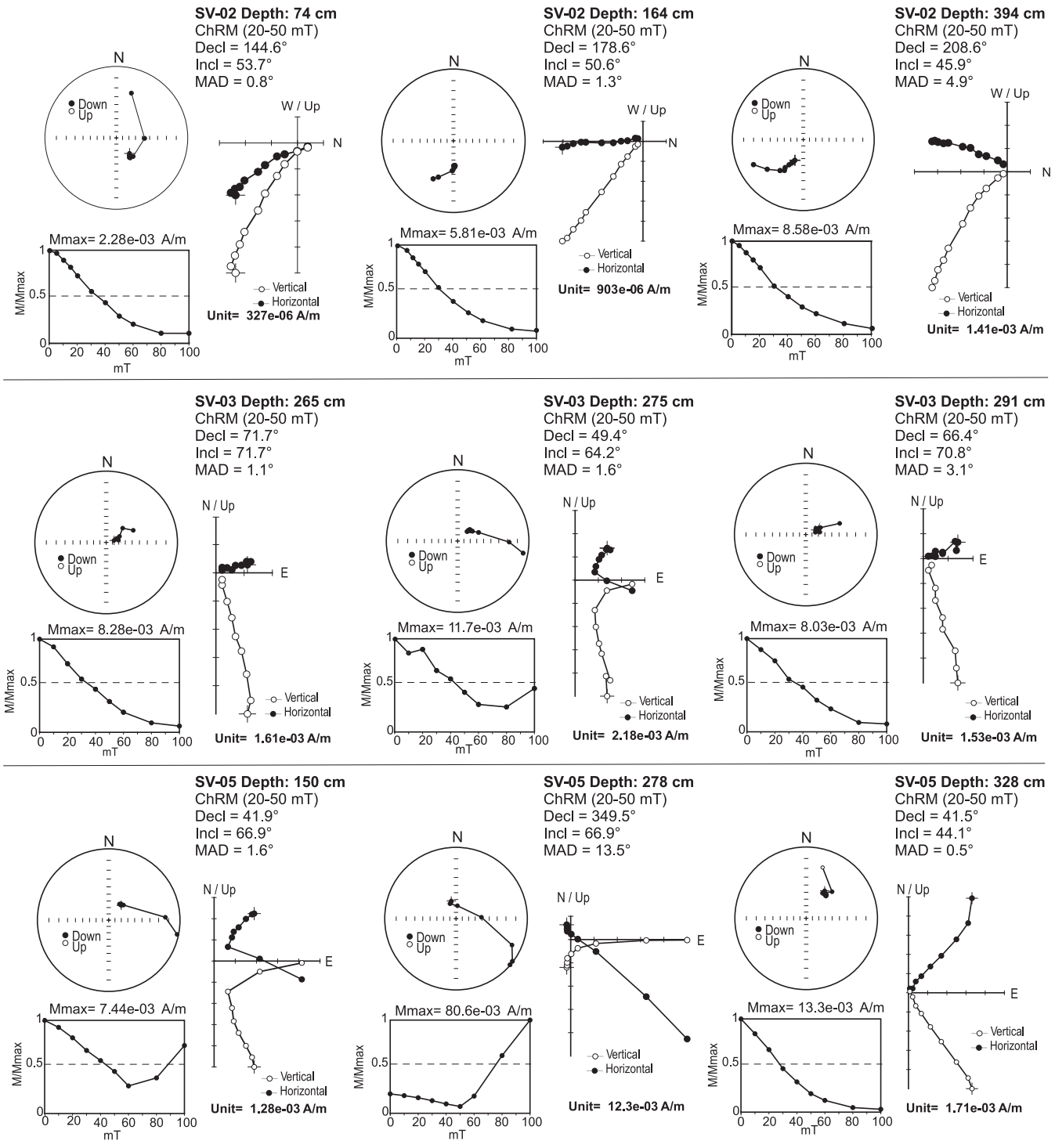

Figure 3. Representative NRM demagnetization orthogonal vector diagrams for selected specimens subjected to AF demagnetization. A ChRM is well defined in all samples by linear paths towards the origin. Some samples (e.g. depth 150 cm and depth 278 cm in core SV-05) are characterized by a marked acquisition of a spurious gyromagnetic remanent magnetization in AF peaks >50 mT.

latitude (about 75°N) of the sampling sites. Since the cores were not azimuthally oriented, the ChRM declination trends for each u-channel have been arbitrarily rotated, so to align their average value of with true north. We refer therefore to ChRM 'relative declination' values in the plots of Figs 4(b) and 5. The ChRM declination values show limited variation (mostly in the range ±10°) in cores SV-02 and SV-03, whereas larger variation are observed in core SV-05, especially for the uppermost part of the plumites interval (about 40–120 cm depth), where ChRM inclination values are higher than elsewhere (mostly in the range 75–85°) and vary around the GAD prediction of 82° (Figs 4b and 5).

Relative palaeointensity (RPI) trends have been estimated by normalizing the NRM intensity measured at various demagnetization steps (0, 20 and 40 mT) by the corresponding ARM intensity values measured at the same AF steps ($NRM_{xx\ mT}/ARM_{xx\ mT}$), as well as by the corresponding magnetic susceptibility values ($NRM_{xx\ mT}/k$).

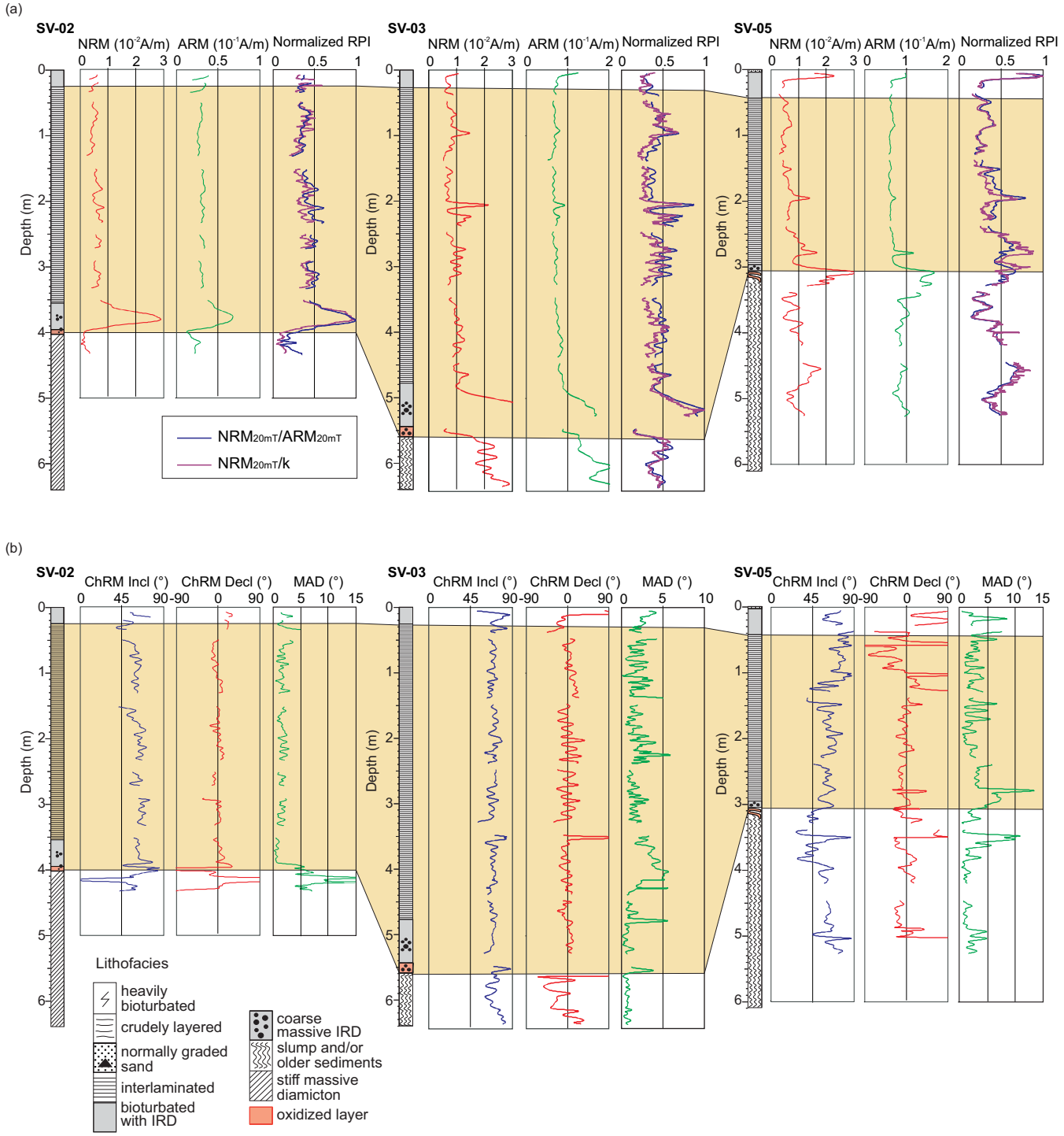

Figure 4. (a) Downcore variation of the main concentration-dependent rock magnetic parameters measured for the analysed cores (NRM, natural remanent magnetization; ARM, anhysteretic remanent magnetization) and of the computed relative palaeointensity (RPI) trends. (b) Downcore variation of the palaeomagnetic data for the analysed cores (ChRM, characteristic remanent magnetization; Decl, relative declination; Incl, inclination; MAD, maximum angular deviation). The deglaciation interval is coloured in brown.

All the computed RPI trends, scaled to unit maximum, are shown in Figs 4(a) and 5. They are consistent between each other and indicate limited variation in the plumites interval, whereas there is a distinct increase in the underlying massive IRD interval and OX-2 layer. This increase most likely represents the effect of the lithologic change rather that a true geomagnetic field behaviour (Fig. 4). A prerequisite for reliable RPI estimates, in fact, is a verified homogeneity in the lithological character of the sediments and in their magnetic mineralogy (in terms of concentration, composition and grain size; see Tauxe 1993). A possible reason for the higher RPI values in this interval is that k and ARM under normalize NRM variations as a result of a coarser magnetic grain size. Conversely, the verified magnetic and lithologic homogeneity in the finely laminated plumites interval, the general agreement between the different

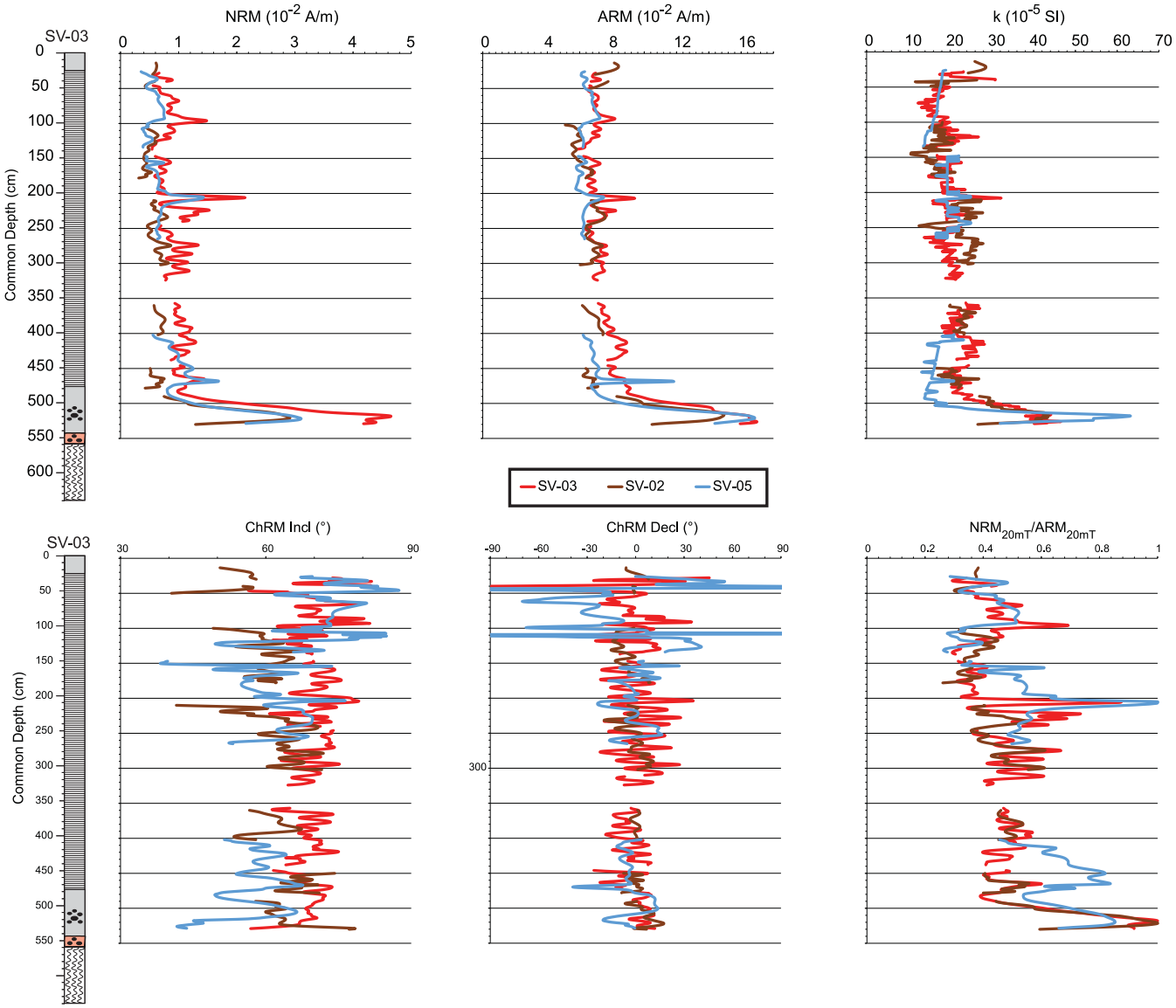

Figure 5. Stratigraphic trends of rock magnetic and palaeomagnetic parameters for the SV-03, SV-02 and SV-05 cores plotted on a common depth scale. Stratigraphic depths of SV-02 and SV-05 were transferred to the SV-03 depth using linear interpolation between tie-points determined from the NRM, ARM and *k* trends. NRM, natural remanent magnetization; ARM, anhysteretic remanent magnetization; k, magnetic susceptibility; ChRM Incl, inclination of the characteristic remanent magnetization, ChRM Decl, declination of the characteristic remanent magnetization; NRM_{20mT}/ARM_{20mT}, relative palaeointensity curves estimated by the NRM/ARM ratio at the 20 mT AF step, with values scaled to unit maximum.

RPI curves and their limited variation suggest that in this interval the reconstructed RPI trends may be considered as reliable estimates of true geomagnetic field variation.

The computed MDF_{NRM} values and mostly vary between 30 and 40 mT (Fig. 6) in all cores. The MDF_{ARM} values also vary in the same range of MDF_{NRM} for cores SV-03 and SV-05, whereas in core SV-02 they are comprised between 25 and 30 mT, which is the range of variability typical for magnetite (Maher 1988). The acquisition of a spurious GRM at high AF steps is virtually absent in core SV-02 and for a large part of core SV-03 (Fig. 6). Instead, various levels in core SV-05 (Fig. 6) show a marked GRM acquisition in AF peaks >50 mT. The ΔGRM/ΔNRM parameter is a sensitive proxy for the occurrence of ferrimagnetic greigite (Fu *et al*. 2008; Sagnotti *et al*. 2010; Liu *et al*. 2014), since the magnitude of GRM acquisition in greigite is larger than in any other known naturally occurring magnetic mineral (Stephenson & Snowball 2001; Roberts *et al*. 2011). The occurrence of greigite in the intervals characterized by high GRM acquisition is also indicated by hysteresis properties (Fig. 7). The hysteresis data point out the prevalence of single domain (SD) magnetic particles with a significant magnetic interaction and a coercivity distribution with a main peak between 60 and 80 mT (Fig. 7). These properties are typical of SD greigite (Roberts *et al*. 2006, 2011; Sagnotti *et al*. 2010).

DISCUSSION

The distribution of the virtual geomagnetic poles (VGPs), calculated by individual ChRM directions under the assumption of a GAD field, is often used to study short-term geomagnetic field behaviour and PSV (see Deenen *et al*. 2011 for a recent review). The scatter of VGPs is usually expressed by the scatter 'S' parameter that indicates the angular standard deviation of the VGP distribution. Sharp and

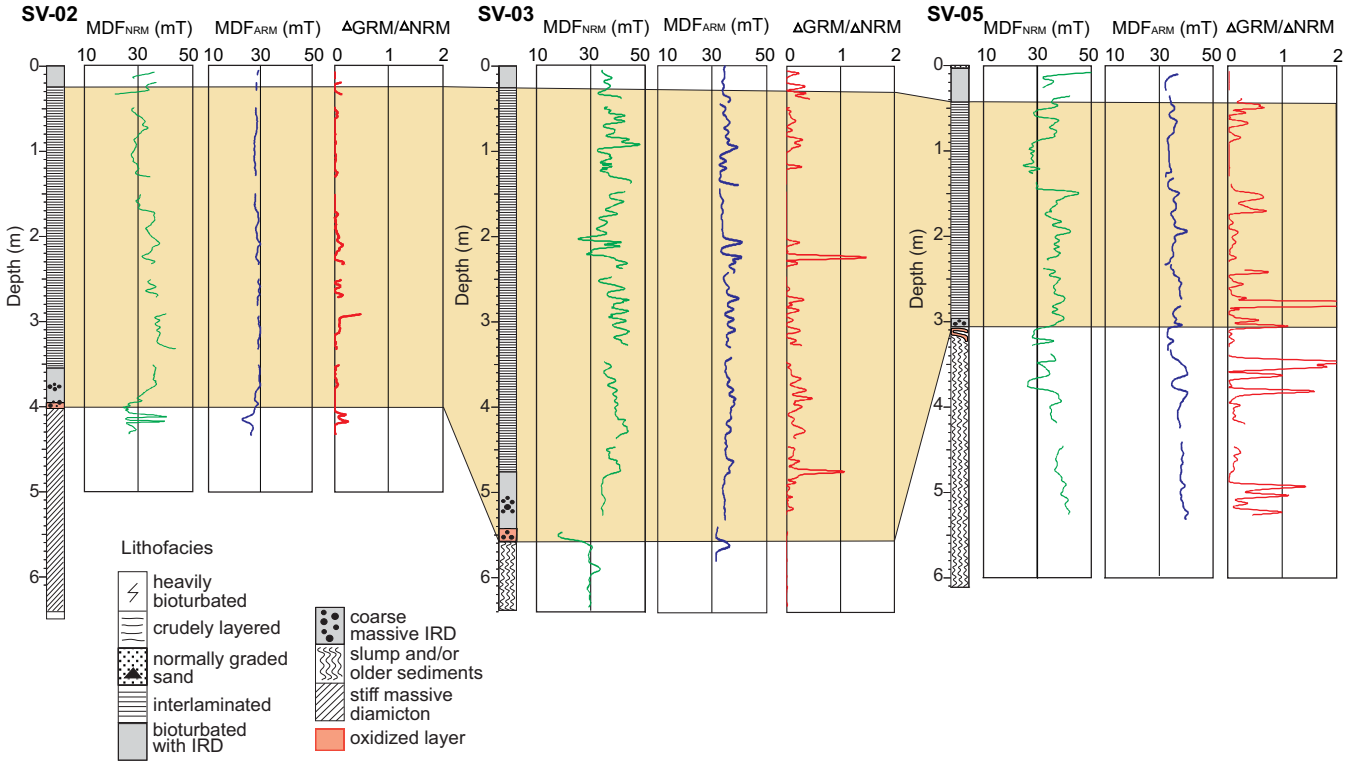

Figure 6. Downcore variation of coercivity-dependent rock magnetic data (MDF_{NRM} and MDF_{ARM}) and of the ΔGRM/ΔNRM parameter for the analysed cores. The deglaciation interval is coloured in brown.

rapid geomagnetic features such as excursions, aborted reversal or polarity transitions are not considered to belong to regular secular variation (SV; e.g. Gubbins 1999; Laj & Channell 2007). In order to filter out large deviations from the mean VGP, it has been proposed to exclude data with large angular deviations from the PSV analysis, on the basis of a fixed cut-off angle (typically of 45°) or on a variable cut-off angle computed by an iterative approach (Vandamme 1994).

In this study, we exploited a unique opportunity to study PSV and VGP scatter at ultra-high-resolution at polar northern latitudes during a time interval spanning a couple of centuries. This is the time interval represented by the interlaminated plumites of Lucchi *et al*. (2013), which were associated to rapid deposition under extensive subglacial outbursts of turbid meltwaters in response to rapid ice sheet melting and retreat during the last deglaciation. This stratigraphic interval has a thickness of various meters in the upper slope cores (up to 4.5 m in core SV-03, proximal area) while it is only 20–30-cm-thick in the cores recovered in the middle slope (core SV-04 and EG-02, Sagnotti *et al*. 2011b; Lucchi *et al*. 2013) representing the distal depositional area in the sedimentary system. According to radiocarbon ages, this interval deposited between about 14 929 (±141) Cal. a BP and 15 061 (±146) Cal. a BP. The age assignment of the interlaminated plumites recovered in the studied cores, present two main problems to overcome: (1) the difficulties encountered in dating terrigenous, barren sediments and (2) the short age range assigned to this interval (about 130 a) that is comparable with the calibrated age errors (about 140 a). The crono-stratigraphic assignment was constrained through a reliable palaeomagnetic and litho-stratigraphic correlation with the sedimentary sequences described west of Svalbard and neighbouring glacial depositional systems, in which radiocarbon ages are consistent with the timing of MWP-1a indicated in tropical areas (Lucchi *et al*. 2013). The slightly different ages measured in the studied cores (15 061 ± 146–14 929 ± 141 Cal. a BP instead of 14 650–14 310 Cal. a BP, determined by Deschamps *et al*. 2012 offshore Tahiti), were related to underestimation of the local regional reservoir correction applied to radiocarbon dating calibration (see discussion in Lucchi *et al*. 2013). In addition, we point out that the MWP-1a was driven by ice-melting at the high-latitudes, so the studied deposits could represent the inception of such huge palaeoclimatic event.

The use of sediments VGP scatter cannot be used as dating method, but it can certainly help to identify the existence of short-living events independently from their stratigraphic assignment. In the plumites interval, the VGP scatter computed from ChRM directions of SV-02 is limited, with an S value of 9.3° (Fig. 8a). The VGP scatter from the plumites interval of core SV-03 is also low, with an *S* value of 10° when all the data are taken into account, which reduces to 8.5° when the Vandamme (1994) iterative cut method is applied in order to filter out large variations from the mean VGP (Fig. 8b). The VGP scatter is distinctly higher in the plumites interval of core SV-05, with an *S* value of 15.8° (Fig. 8c).

Various geomagnetic field models predict that *S* should increase with latitude (e.g. model G, McElhinny & McFadden 1997; model TK03.GAD of Tauxe & Kent 2004) in a range varying from about 9° to about 23°. According to the TK03.GAD model, at the latitude of the study area regular SV should result in a *S* value of about 23° with no cut-off criterion and of about 17° when the Vandamme iterative cut-off method is applied (Fig. 9). However, a compilation of palaeomagnetic data from globally distributed lava flows erupted during the last 5 Ma (Johnson *et al*. 2008) suggests that this latitudinal variation appears less large than predicted (Fig. 9), with an estimated *S* value of about 19° for sites at high latitude (>70°). The Holocene palaeomagnetic record obtained from the sedimentary cores retrieved from the middle slope of the Storfjorden and Kveithola TMFs and the adjacent

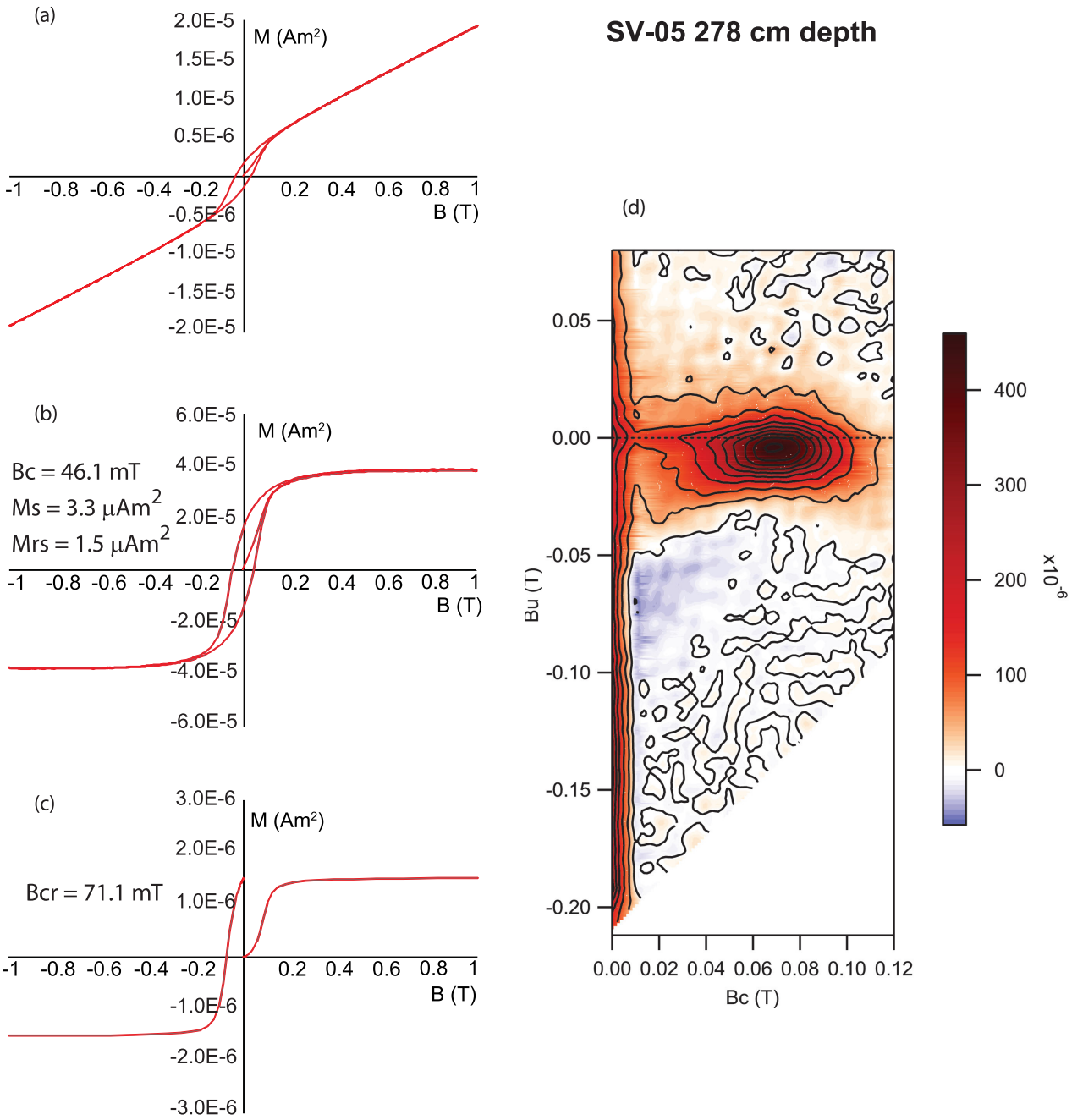

Figure 7. Hysteresis measurements carried out on samples from the interval showing the largest ΔGRM/ΔNRM value (at cm 278 depth in core SV-05). (a) Hysteresis loop measured up to ±1 T. (b) Hysteresis loop after subtraction of the paramagnetic slope, with computed parameters (Bc, coercivity, Ms, saturation magnetization, Mrs, saturation remanent magnetization). (c) Mrs acquisition curves and backfield remagnetization curves up to ±1 T. (d) First order reversal curve (FORC) diagram, computed using the FORCinel software developed by Harrison & Feinberg (2008). It shows concentric contours with a main peak between 60 and 80 mT and a large vertical spread. The vertical spread of this FORC distribution is a manifestation of magnetic interaction, as well as the offset of the FORC distribution below the Bu = 0 axis. All these properties are indicative of single domain greigite (Roberts *et al*. 2006, 2011; Sagnotti *et al*. 2010).

continental shelf indicates a fairly homogeneous VGP scatter with *S* values of about 16° when no cut-off criterion is applied, which reduce to 7–14° with the cut-off criterion of Vandamme (Sagnotti *et al*. 2011b).

The limited VGP scatter observed in core SV-02 and SV-03 is consistent with a rapid emplacement of the plumites, confirming the existence of a very short event as indicated by radiocarbon dating.

The alignment of particle magnetic moments to the ambient magnetic field and their immobilization (lock-in) is controlled by a variety of depositional and post-depositional processes, mostly due to dewatering and compaction (Verosub 1977). This lock-in process induces a time lag between the sediment age and the palaeomagnetic age at a given depth. The half lock-in depth is defined as the depth at which 50 per cent of the available magnetic momentum has definitively been fixed (Bleil & von Dobeneck 1999). The half

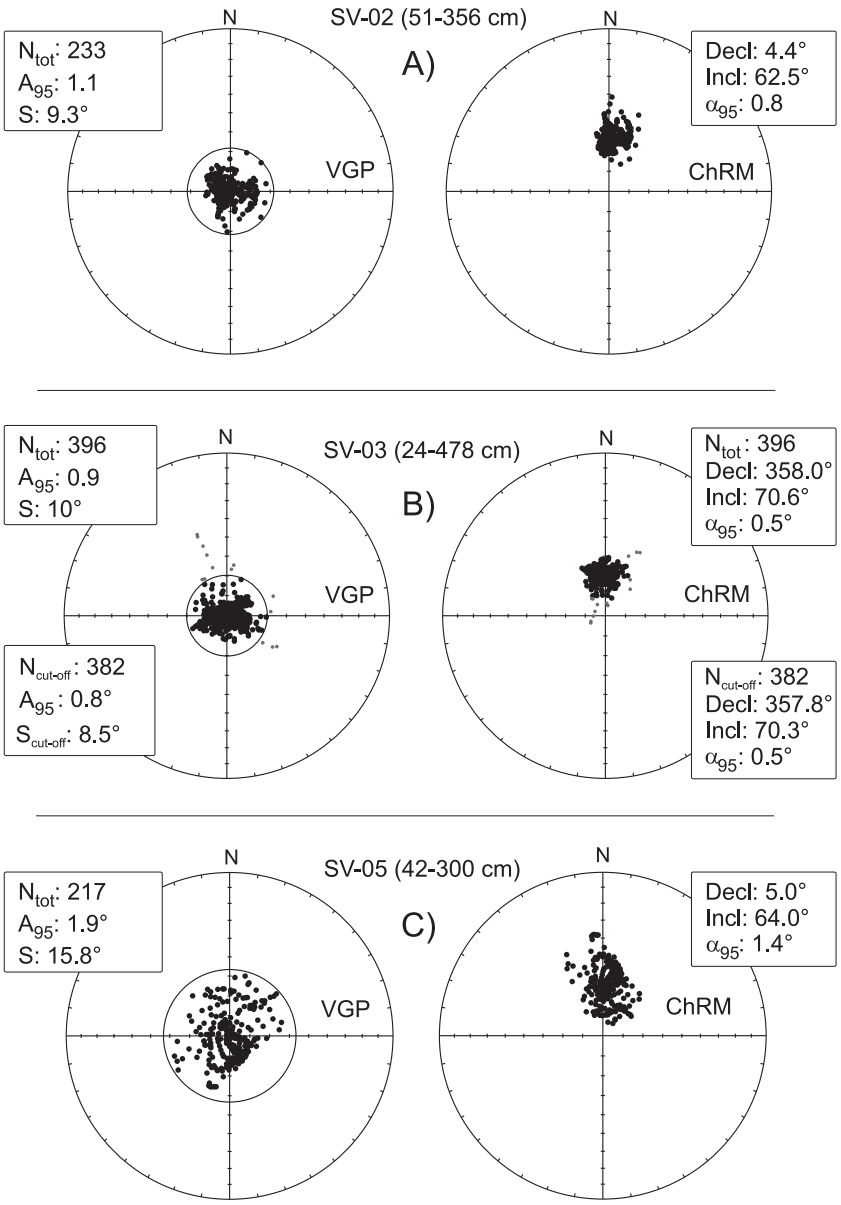

Figure 8. Equal area plots of VGP positions (right-hand side) and ChRM directions (left-hand side) computed for the plumites interval in the SV-02, SV-03 and SV-05 cores. The small circle in the VGP plots indicates the cut-off angle estimated by the Vandamme (1994) method and the grey points outside such small circles indicate the data discarded according to such cut-off angle. N_{tot}, total number of data; A_{95}, half-angle of the 95 per cent confidence cone around the mean VGP; S, VGP scatter; $N_{cut\text{-}off}$, number of data selected according to the Vandamme cut-off; $S_{cut\text{-}off}$, VGP scatter following the application of the Vandamme cut-off; Decl, mean ChRM declination; Incl, mean ChRM inclination; α_{95}, half-angle of the 95 per cent confidence cone around mean ChRM.

lock-in depth varies according to various lock-in functions (constant, linear, Gaussian, cubic, exponential) and in marine sediments it is estimated between 10 and 20 cm below the surface mixed zone (Roberts & Winklhofer 2004; Suganuma *et al*. 2011). The lock-in depth may also vary within the same sedimentary sequence (Sagnotti *et al*. 2005). In any case, rapidly deposited sediments are the less affected by the lock-in processes, so that the age offset between sediments and the palaeomagnetic record may be safely considered minimum for any lock-in function. The wider VGP scatter observed in core SV-05 located at the head-scar of a landslide, may partly reflect possible disturbance around the sediment remanence lock-in depth, as an effect of minor syn-sedimentary, re-depositional events possibly occurred during the plumites emplacement. Re-deposition/small slumps were described in the deeper part of SV-05 core (disturbed oxidized layer OX-2) and can be noted through the radiographs record of the core.

In addition to this argument, we suggest that the observed discrepancy in the VGP scatter record provided by the same stratigraphic interval retrieved in multiple cores may be explained by a slightly asynchronous, or interfering, magnetic remanence acquisition by two distinct populations of magnetic minerals, whose relative proportion varies in the stratigraphic sequence. This is the case of core SV-05, where we observe a variable tendency to acquire a GRM at high fields during the AF demagnetization treatment throughout the core, which can be representative of a variable content of greigite versus magnetite. In fact, in the cores where the magnetic mineralogy is essentially uniform and magnetite is the main magnetic carrier (SV-02 and SV-03) the VGP scatter in the plumites interval

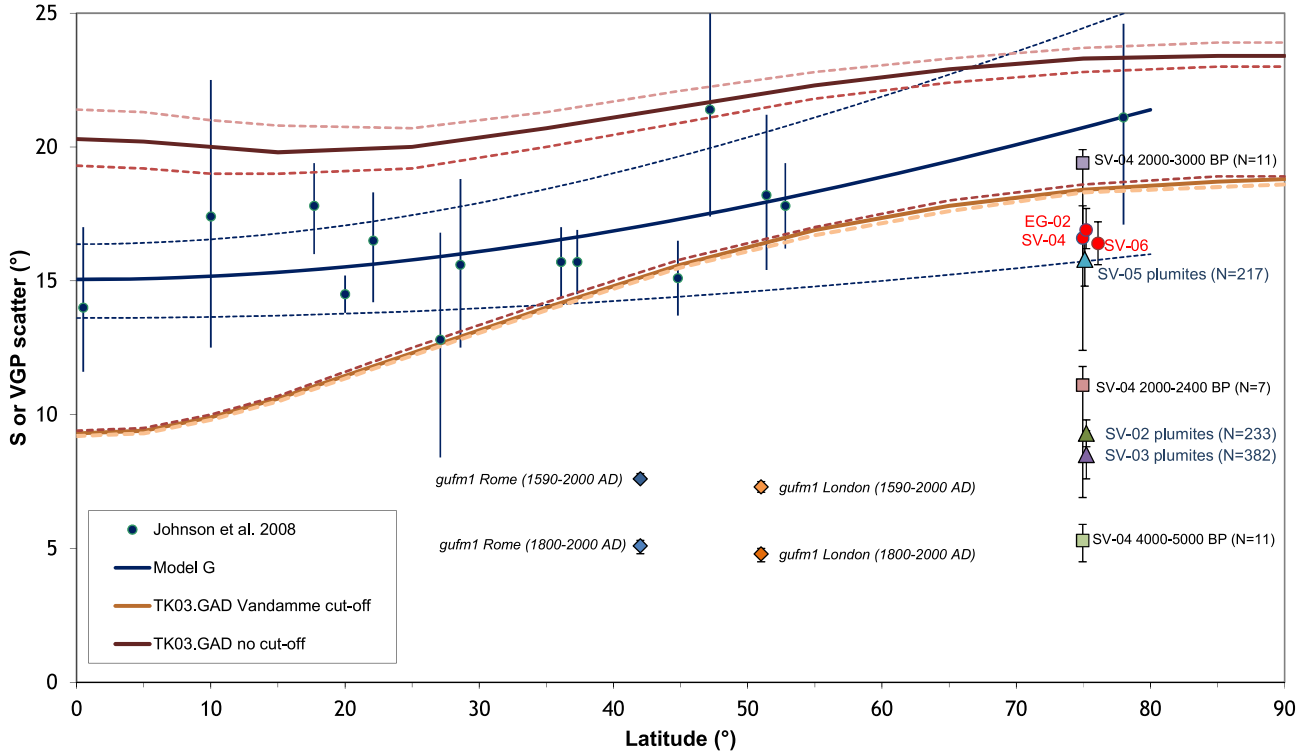

Figure 9. Models of VGP scatter values (S) as a function of geographic latitude. The dots refer the PSV database of Johnson *et al*. (2008) for the last 5 Ma. The reported curves are drawn from the G model of McElhinny & McFadden (1997) and the TK03.GAD model of Tauxe & Kent (2004), computed with and without the cut-off criterion of Vandamme (1994). For model predictions, the dashed lines denote 95 per cent error bounds. The yellow circles indicate the S data obtained in this study for the plumites interval of cores SV-02, SV-03 and SV-05. The data computed for the Holocene interval of the adjacent SVAIS and EGLACOM cores (Sagnotti *et al*. 2011b) are also shown for comparison (red circles).

is considerably lower than expected for a time period long enough to sample the full spectrum of geomagnetic secular variation, with a S value of about 9° (9.3° and 8.9°, respectively). Such S value is consistent with a rapid deposition of this stratigraphic interval, for which the computed 95 per cent confidence cone around the mean VGP (A95) is lower than the lower limit ($A95_{min}$) calculated following the method of Deenen *et al*. (2011) to ascertain whether or not a distribution has sufficiently well-sampled geomagnetic PSV.

We point out that the last four centuries of direct geomagnetic observations indicate a lower VGP scatter due to geomagnetic PSV. As a comparison, we computed the VGP scatter at European mid-latitudes (i.e. the region from which the main part of the historical direct geomagnetic observations were made) by using the *gufm1* global model of Jackson *et al*. (2000). The results indicate that, when considered over the whole time interval (1590–2000 AD) span by the model, the VGP scatter for Rome (latitude of 42°N) and London (latitude of 51°N) is of 7.6° and 7.3°, respectively (Fig. 9). When the computation is made on the last two centuries only (1800–2000 AD), the S value calculated from *gufm1* reduces to 5.1° at Rome and to 4.8° at London (Fig. 9).

Anyway, it must be noted that the VGP scatter at a given latitude may also vary significantly with time. In fact, the Holocene PSV record reconstructed for the NW Barents Sea suggests that intervals of fast PSV alternated with periods of slow PSV (see fig. 10 in Sagnotti *et al*. 2011b). In particular, the VGP scatter computed from data from the SV-04 core markedly increases during centuries of fast PSV, reaching a S value of 11.1° for the 2000–2400 yr BP period and increasing up to 19.4° for the millennium between 2000 and 3000 yr BP. Conversely, during centuries of limited PSV the VGP scatter at the same site is considerably reduced: in core SV-04 we computed a S value of only 5.3° for the millennium between 4000 and 5000 yr BP (Fig. 9). If we assume that the geomagnetic field varied at a rate similar to that measured during the last four centuries, the data from the SV-02 and SV-03 cores indicate that the VGP scatter recorded by the plumites interval (S of about 8–9°) is compatible with its deposition during a time span of a few (4–5) hundred years. This S value may still be compatible with a deposition in less than two centuries, as suggested by the radiocarbon dating, if the rate of PSV at about 15 ka BP was higher than in modern times (e.g. as it occurred in the same region during the period 2–3 ka BP). We also notice that the analysed sediments may have been affected by effects of inclination shallowing due to compaction and dewatering, which could lead to biasing effects that distort the palaeomagnetic directions (e.g. Tauxe & Kent 2004; Tauxe 2005) and therefore to an apparent VGP scatter higher than expected. The possible effects of inclination shallowing provide further support to the conclusion that the plumites interval was deposited by an extremely rapid event. In core SV-05, the additional presence of a magnetic mineral prone to GRM acquisition, most likely greigite, results in a distinctly higher VGP scatter recorded in the same stratigraphic interval, with a $S_{cut\text{-}off}$ value of about 16°. This value is very similar to the S values obtained for the whole Holocene sequence of the adjacent SVAIS and EGLACOM cores (Sagnotti *et al*. 2011b) and may induce to the erroneous conclusion that this stratigraphic interval spans a time period long enough to fully sample PSV, since the computed A95 value about the mean VGP is higher than the $A95_{min}$ value estimated following Deenen *et al*. (2011).

CONCLUSIONS

This study offered the opportunity to investigate in detail the rate of geomagnetic PSV in the high northern latitudes at a decadal scale over a time interval of about two centuries. The data indicate that notwithstanding demagnetization diagrams allow a straightforward determination of the ChRM directions in all the cores, the amplitude of directional PSV is distinctly higher in one core (SV-05) than in the other two cores (SV-02 and SV-03). The analysis of a variety of rock magnetic and palaeomagnetic data indicate that magnetite is the main magnetic carrier in cores SV-02 and SV-03. Conversely, greigite appears to be also present, in addition to magnetite, as main remanence carrier in core SV-05, as indicated by a pronounced tendency for GRM acquisition during AF demagnetization and by the hysteresis properties. We conclude that this latter core is not suitable for PSV analysis due to (1) the presence of a mixed magnetic mineralogy and a downcore variable proportion of magnetic minerals that significantly affected the way and the accuracy with which sediments recorded geomagnetic field variation and (2) the bathymetric location of the core determining a high risk of syn-sedimentary redepositional events (e.g. slumps) during plumites emplacement. The VGP scatter (*S*) computed from palaeomagnetic data of the plumites interval in cores SV-02 and SV-03 is of about 9°. This *S* value is consistent with a fast deposition of the stratigraphic interval represented by the plumites, which according to the available ^{14}C ages spans about two centuries. We therefore conclude that a VGP scatter quantified by a *S* value of about 8–9° could be considered as a reliable approximation of geomagnetic secular variation effects at a latitude of 75°N over the analysed couple of centuries. Reconstruction of the sediment VGP scatter resulted to be an original tool for the identification of short-living depositional events. This method, applied in synergy with dating techniques, can help overcoming many stratigraphic uncertainties.

ACKNOWLEDGEMENTS

This study was supported by the Italian projects PNRA-CORIBAR (PdR 2013/C2.01) and Premiale ARCA, and the Spanish IPY project DEGLABAR (CTM2010-17386). We thank the scientific party and crew of the SVAIS (POL2006-07390/CGL) and OGS-EGLACOM Arctic expeditions for data acquisition. We are also grateful to the Editor and two anonymous Reviewers for comments and suggestions that greatly improved the manuscript.

REFERENCES

Biggin, A.J., Strik, G.H. & Langereis, C.G., 2008. Evidence for a very-long-term trend in geomagnetic secular variation, *Nat. Geosci.,* **1**(6), 395–398.

Bleil, U. & von Dobeneck, T., 1999. Geomagnetic events and relative paleointensity records—clues to high-resolution paleomagnetic chronostratigraphies of Late Quaternary marine sediments?, in *Use of Proxies in Paleoceanography: Examples from the South Atlantic,* pp. 635–654, eds Fischer, G. & Wefer, G., Springer.

Bloxham, J. & Gubbins, D., 1985. The secular variation of Earth's magnetic field, *Nature,* **317,** 777–781.

Bullard, E.C., 1948. The secular change in the earth's magnetic field, *Mon. Not. R. Astron. Soc., Geophys. Suppl.,* **5,** 248–257.

Constable, C.G. & Parker, R.L., 1988. Statistics of the geomagnetic secular variation for the past 5 m.y., *J. geophys. Res.,* **93**(B10), 11 569–11 581.

Cox, A., 1970. Latitude dependence of the angular dispersion of the geomagnetic field, *Geophys. J. R. astr. Soc.,* **20,** 253–269.

Creer, K.M., 1962. The dispersion of the geomagnetic field due to secular variation and its determination for remote times from palaeomagnetic data, *J. geophys. Res.,* **67**(9), 3461–3476.

Creer, K.M., 1981. Long-period geomagnetic secular variations since 12 000 yr BP, *Nature,* **292**(5820), 208–212.

Creer, K.M., Irving, E. & Nairn, A.E.M., 1959. Palaeomagnetism of the Great Whin Sill, *Geophys. J. R. astr. Soc.,* **2,** 306–323.

Deenen, M.H., Langereis, C.G., van Hinsbergen, D.J. & Biggin, A.J., 2011. Geomagnetic secular variation and the statistics of palaeomagnetic directions, *Geophys. J. Int.,* **186**(2), 509–520.

Deschamps, P. *et al.*, 2012. Ice-sheet collapse and sea-level rise at the Bølling warming 14 600 years ago, *Nature,* **483,** 559–564.

Fu, Y., von Dobeneck, T., Franke, C., Heslop, D. & Kasten, S., 2008. Rock magnetic identification and geochemical process models of greigite formation in Quaternary marine sediments from the Gulf of Mexico (IODP Hole U1319A), *Earth planet. Sci. Lett.,* **275,** 233–245.

Gubbins, D., 1999. The distinction between geomagnetic excursions and reversals, *Geophys. J. Int.,* **137,** F1–F3.

Hagstrum, J.T. & Champion, D.E., 2002. A Holocene palaeosecular variation record from 14C-dated volcanic rocks in western North America, *J. geophys. Res.,* **107**(B1), 2025, doi:10.1029/2001JB000524.

Harrison, R.J. & Feinberg, J.M., 2008. FORCinel: an improved algorithm for calculating first-order reversal curve distributions using locally weighted regression smoothing, *Geochem. Geophys. Geosyst.,* **9,** Q05016, doi:10.1029/2008GC001987.

Hesse, R., Khodabakhsh, S., Klauck, I. & Ryan, W.B.F., 1997. Asymmetrical turbid surface-plume deposition near ice-outlets of the Pleistocene Laurentide ice sheet in the Labrador Sea, *Geo-Mar. Lett.,* **17,** 179–187.

Holcomb, R., Champion, D. & McWilliams, M., 1986. Dating recent Hawaiian lava flows using palaeomagnetic secular variation, *Geol. Soc. Am. Bull.,* **97**(7), 829–839.

Holme, R. & Olsen, N., 2006. Core surface flow modelling from high-resolution secular variation, *Geophys. J. Int.,* **166,** 518–528.

Jackson, A., Jonkers, R.T. & Walker, M.R., 2000. Four centuries of geomagnetic secular variation from historical records, *Phil. Trans. R. Soc. Lond., A,* **358,** 957–990.

Johnson, C.L. *et al.*, 2008. Recent investigations of the 0–5 Ma geomagnetic field recorded by lava flows, *Geochem. Geophys. Geosyst.,* **9**(4), doi:10.1029/2007GC001696.

Kirschvink, J.L., 1980. The least-squares line and plane and the analysis of palaeomagnetic data, *Geophys. J. Int.,* **62**(3), 699–718.

Laberg, J.S. & Vorren, T.O., 1996. The glacier-fed fan at the mouth of Storfjorden trough, western Barren Sea: a comparative study, *Geol. Rundsch.,* **85,** 338–349.

Laj, C. & Channell, J.E.T., 2007. Geomagnetic excursions, *Treatise geophys.,* **5**(373), e416.

Liu, J. *et al.*, 2014. Magnetostratigraphy of a greigite-bearing core from the South Yellow Sea: implications for remagnetization and sedimentation, *J. geophys. Res.: Solid Earth,* **119,** doi:10.1002/2014JB011206.

Lucchi, R.G. & Rebesco, M., 2007. Glacial contourites on the Antarctic Peninsula margins: insight for palaeoenvironmental and palaeoclimatic conditions, in *Economic and Palaeosignificance of Contourite Deposits,* Vol. 276, pp. 111–127, eds Viana, A.R. & Rebesco, M., Geological Society of London, Special Publication.

Lucchi, R.G. *et al.*, 2002. Glacimarine sedimentary processes of a high-latitude, deep-sea sediment drift (Antarctic Peninsula Pacific margin), *Mar. Geol.,* **189,** 343–370.

Lucchi, R.G. *et al.*, 2013. Postglacial sedimentary processes on the Storfjorden and Kveithola trough mouth fans: impact of extreme glacimarine sedimentation, *Global planet. Changes,* **111,** 309–326.

Lund, S.P., 1985. A comparison of the statistical secular variation recorded in some late Quaternary lava flows and sediments, and its implications, *Geophys. Res. Lett.,* **12**(5), 251–254.

Maher, B.A., 1988. Magnetic properties of some synthetic sub-micron magnetites, *Geophys. J. Int.,* **94**(1), 83–96.

Mangerud, J. & Gulliksen, S., 1975. Apparent radiocarbon ages of recent marine shells from Norway, Spitsbergen, and Arctic Canada, *Quarter. Res.,* **5,** 263–273.

McElhinny, M.W. & McFadden, P.L., 1997. Palaeosecular variation over the past 5 Myr based on a new generalized database, *Geophys. J. Int.,* **131**(2), 240–252.

McFadden, P.L., Merrill, R.T. & McElhinny, M.W., 1988. Dipole/quadrupole family modeling of palaeosecular variation, *J. geophys. Res.,* **93**(B10), 11 583–11 588.

Rebesco, M. *et al.*, 2013. Contourite drifts of the Western Spitsbergen margin, *Deep-Sea Res. I,* **79,** 156–168.

Reimer, P.J. *et al.*, 2009. IntCal09 and Marine09 radiocarbon age calibration curves, 0–50 000 years cal BP, *Radiocarbon,* **51,** 1111–1150.

Roberts, A.P., 2006. High-resolution magnetic analysis of sediment cores: strengths, limitations and strategies for maximizing the value of long-core magnetic data, *Phys. Earth planet. Inter.,* **156,** 162–178.

Roberts, A.P. & Winklhofer, M., 2004. Why are geomagnetic excursions not always recorded in sediments? Constraints from post-depositional remanent magnetization lock-in modelling, *Earth planet. Sci. Lett.,* **227,** 345–359.

Roberts, A.P., Liu, Q., Rowan, C.J., Chang, L., Carvallo, C., Torrent, J. & Horng, C.S., 2006. Characterization of hematite (α-Fe_2O_3), goethite (α-FeOOH), greigite (Fe_3S_4), and pyrrhotite (Fe_7S_8) using first-order reversal curve diagrams, *J. geophys. Res.: Solid Earth (1978–2012),* **111**(B12), doi:10.1029/2006JB004715.

Roberts, A.P., Chang, L., Rowan, C.J., Horng, C.S. & Florindo, F., 2011. Magnetic properties of sedimentary greigite (Fe_3S_4): an update, *Rev. geophys.,* **49**(1), doi:10.1029/2010RG000336.

Sagnotti, L., 2013. Demagnetization Analysis in Excel (DAIE)—an open source workbook in Excel for viewing and analyzing demagnetization data from paleomagnetic discrete samples and u-channels, *Ann. Geophys.,* **56,** D0114, doi:10.4401/ag-6282.

Sagnotti, L., Rochette, P., Jackson, M., Vadeboin, F., Dinarès-Turell, J., Winkler, A. & "Mag-Net" Science Team, 2003. Inter-laboratory calibration of low field and anhysteretic susceptibility measurements, *Phys. Earth Planet. Int.,* **138,** 25–38.

Sagnotti, L., Budillon, F., Dinarès-Turell, J., Iorio, M. & Macrì, P., 2005. Evidence for a variable paleomagnetic lock-in depth in the Holocene sequence from the Salerno Gulf (Italy): implications for "high-resolution" paleomagnetic dating, *Geochem. Geophys. Geosyst.,* **6**(11), doi:10.1029/2005GC001043.

Sagnotti, L., Cascella, A., Ciaranfi, N., Macrì, P., Maiorano, P., Marino, M. & Taddeucci, J., 2010. Rock magnetism and palaeomagnetism of the Montalbano Jonico section (Italy): evidence for late diagenetic growth of greigite and implications for magnetostratigraphy, *Geophys. J. Int.,* **180**(3), 1049–1066.

Sagnotti, L. *et al.*, 2011a. A continuous palaeosecular variation record of the last 4 millennia from the Augusta Bay (Sicily, Italy), *Geophys. J. Int.,* **184,** 191–202.

Sagnotti, L., Macrì, P., Lucchi, R., Rebesco, M. & Camerlenghi, A., 2011b. A Holocene palaeosecular variation record from the northwestern Barents Sea continental margin, *Geochem. Geophys. Geosyst.,* **12,** Q11Z33, doi:10.1029/2011GC003810.

Snowball, I., Zillén, L., Ojala, A., Saarinen, T. & Sandgren, P., 2007. FENNOSTACK and FENNORPIS: varve dated Holocene palaeomagnetic secular variation and relative palaeointensity stacks for Fennoscandia, *Earth planet. Sci. Lett.,* **255,** 106–116.

Speranza, F., Pompilio, M., D'Ajello Caracciolo, F. & Sagnotti, L., 2008. Holocene eruptive history of the Stromboli volcano: constraints from paleomagnetic dating, *J. geophys. Res.,* **113,** B09101, doi:10.1029/2007JB005139.

Stephenson, A. & Snowball, I.F., 2001. A large gyromagnetic effect in greigite, *Geophys. J. Int.,* **145**(2), 570–575.

Stuiver, M. & Reimer, P.J., 1993. Extended 14C database and revised CALIB radiocarbon calibration program, *Radiocarbon,* **35,** 215–230.

Suganuma, Y., Okuno, J.I., Heslop, D., Roberts, A.P., Yamazaki, T. & Yokoyama, Y., 2011. Post-depositional remanent magnetization lock-in for marine sediments deduced from 10 Be and paleomagnetic records through the Matuyama–Brunhes boundary, *Earth planet. Sci. Lett.,* **311**(1), 39–52.

Tanguy, J.-C., Bucur, I. & Thompson, J.F.C., 1985. Geomagnetic secular variation in Sicily and revised ages of historic lavas from Mount Etna, *Nature,* **318,** 453–455.

Tauxe, L., 1993. Sedimentary records of relative paleointensity of the geomagnetic field: theory and practice, *Rev. geophys,* **31**(3), 319–354.

Tauxe, L., 2005. Inclination flattening and the geocentric axial dipole hypothesis, *Earth planet. Sci. Lett.,* **233**(3), 247–261.

Tauxe, L. & Kent, D.V., 2004. A simplified statistical model for the geomagnetic field and the detection of shallow bias in palaeomagnetic inclinations: was the ancient magnetic field dipolar, *Geophys. Monogr.,* **145,** 101–116.

Taylor, J., Dowdeswell, J.A., Kenyon, N.H. & Cofaigh, C.Ò., 2002. Late Quaternary architecture of trough-mouth fans: debris flows and suspended sediments on the Norwegian margin, in *Glacially-Influenced Sedimentation on High-Latitude Continental Margins,* eds Dowdeswell, J.A. & Cofaigh, Ó.C., Vol. 203, pp. 55–71, Geological Society of London, Special Publications.

Thompson, R. & Barraclough, D.R., 1982. Geomagnetic secular variation based on spherical harmonic and cross validation analyses of historical and archaeomagnetic data, *J. Geomagn. Geoelectr.,* **34,** 245–263.

Turner, G.M. & Thompson, R., 1981. Lake sediment record of the geomagnetic secular variation in Britain during Holocene times, *Geophys. J.,* **65,** 703–725.

Turner, G.M. & Thompson, R., 1982. Detransformation of the British geomagnetic secular variation record for Holocene times, *Geophys. J.,* **70,** 789–792.

Vandamme, D., 1994. A new method to determine palaeosecular variation, *Phys. Earth planet. Inter.,* **85,** 131–142.

Verosub, K.L., 1977. Depositional and postdepositional processes in the magnetization of sediments, *Rev. Geophys.,* **15,** 129–143.

Verosub, K.L., 1988. Geomagnetic secular variation and the dating of Quaternary sediments, *Geol. Soc. Am. Spec. Pap.,* **227,** 123–138.

Vorren, T.O. & Laberg, J.S., 1997. Trough mouth fans–palaeoclimate and ice-sheet monitors, *Quater. Sci. Rev.,* **16,** 865–881.

Weeks, R., Laj, C., Endignoux, L., Fuller, M., Roberts, A., Manganne, R., Blanchard, E. & Goree, W., 1993. Improvements in long-core measurement techniques: applications in palaeomagnetism and palaeoceanography, *Geophys. J. Int.,* **114,** 651–662.